

Frequency-Dependent and Full Range Tunable Phase Shifter

Yufu Yin, Tao Lin, Shanghong Zhao, Zihang Zhu, Xuan Li, Wei Jiang, Qirong Zheng, Hui Wang

Abstract—In this paper, a frequency-dependent and tunable phase shifter is proposed and numerically analyzed. The key devices are the dual-polarization binary phase shift keying modulator (DP-BPSK) and the fiber Bragg grating (FBG). The phase-frequency response of the FBG is employed to determine the frequency-dependent phase shift. The simulation results show that a linear phase shift of the recovered output microwave signal which depends on the frequency of the input RF signal is achieved. In addition, by adjusting the power of the RF signal, the full range phase shift from 0° to 360° can be realized. This structure shows the spurious free dynamic range (SFDR) of $70.90 \text{ dB}\cdot\text{Hz}^{2/3}$ and $72.11 \text{ dB}\cdot\text{Hz}^{2/3}$ under different RF powers.

Keywords—Microwave photonics, phase shifter, spurious free dynamic range, frequency-dependent.

I. INTRODUCTION

MICROWAVE photonics (MWP) technology combines the advantages of electrical technology and the superiorities of optical technology. The drawbacks of limit operation bandwidth, electromagnetic interference (EMI), bulk structure, large weight and low isolation in the electrical field can be well overcome by the MWP technology [1], [2]. It is hitherto widely employed in the communication systems and radar system, especially the MWP phase shifter. It is one of the significant components which guarantee that the phase array radar performs the beam steering electrically without mechanical movement.

In recent years, various kinds of MWP phase shifter are presented [2]-[10]. For example, the full range phase shift can be achieved by adjusting the optical wavelength [3], [4] or the optical power [5]. The dual-sideband phase-control-based structure can be employed to achieve the large range phase shift in the recovered microwave signal [6]. Polarization state dependent [7], [8] or RF amplitude dependent [9] phase shifters are recently reported. The stimulated Brillouin scattering (SBS) is also used to realize the phase shift [10], [11]. Besides, the electro-optic modulators (EOM) based phase shifters are also widely researched [12], [13] due to the convenient phase tuning by the DC bias voltage altering. Although the aforementioned method can achieve the full range and stable phase shifting, it still faces the non-ignorable problem in the phase array system. Because of the restriction of aperture effect and the aperture

Yufu Yin, Tao Lin, Shanghong Zhao, Zihang Zhu, Xuan Li, Qirong Zheng and Hui Wang are with the Air Force Engineering University, College of Information and Navigation, Xi'an 710077, China (e-mail: 503246705@qq.com, ltzhineng@126.com, zhaoshangh@aliyun.com, zhuzihang6@126.com, lixuanrch@163.com, zqr1620@sina.com, 1012918865@qq.com).

Wei Jiang is now with the National Key Laboratory of Science and Technology on Space Microwave, Xi'an 710077, China (e-mail: tsingh504@163.com).

traverse delay, it is difficult for the conventional phase array radar to get the wide instantaneous bandwidth under wide scan scope. According to the principle of beam pointing, $\varphi=2\pi d(f_0-\Delta f)\sin(\theta_0+\Delta\theta)c$. Here, φ is the phase shift, d is the antenna interval, f_0 and Δf are the initial frequency and the frequency deviation respectively, θ_0 and $\Delta\theta$ are the initial beam pointing direction and the pointing deviation, respectively. It can be figured that the phase shift should linearly respond to frequency so that the beam pointing can be well maintained. Traditionally, the problem can be well solved by the optical true time delay [14], [15]. However, the time delay greatly depends on the specially required fiber length which is hard to guarantee due to the extra high frequency of the lightwave.

In this paper, a distinctive frequency-dependent and full range tunable phase shifter based on the phase-frequency response of the FBG is proposed. The structure is compact for only one integrated modulator of DP-BPSK, and one commercial FBG is employed. Because of the limit experimental condition, the theoretical analysis is shown firstly, and then, the simulation work is taken by the software of "Optisystem" to verify the proposed method.

II. PRINCIPLE

Fig. 1 shows the proposed schematic of frequency dependent phase shifter. It consists of a DP-BPSK and a FBG. In this structure, the laser diode (LD) launches a lightwave with the angular frequency of ω_c and the amplitude of E_c . In order to simplify the theoretical analysis, the lightwave is regarded as a strict sinusoidal waveform and can be expressed as $E_c(t)=E_c\cos\omega_c t$. It is first led to the DP-BPSKM, which integrates two dual driven Mach-Zehnder modulators (DMZMx and DMZMy), a 90-degree polarization rotator and a polarization beam combiner (PBC). The DMZM is another kind of integrated modulator that integrates two phase modulators (PM) in a main Mach-Zehnder modulator (MZM). There are two RF ports (Uport and Lport) and one DC bias port in a DMZM. The DP-BPSKM is driven by an RF signal $V_{RF}(t)=V_{RF}\sin\omega_{RF}t$. Here, V_{RF} and ω_{RF} are the amplitude and the angular frequency of the RF signal, respectively. It is equally split into two paths (up-path and low-path). The up-path is split and phase shifted by the 90° hybrid coupler to drive the two PMs in the DMZMx through Uport and Lport, respectively. In order to perform the single sideband modulation, the DCx bias voltage is set to be $-\pi/2$. Under the small signal modulation, the higher order sidebands can be ignored. Hence, the output signal of the DMZM after driven by the RF can be expressed as

$$\begin{aligned}
 E_{DMZMx}(t) &= E_c(t) \left[\exp\left(j \frac{A_x V_{RF}}{4} \sin \omega_{RF} t\right) + \exp\left(j \frac{A_x V_{RF}}{4} \cos \omega_{RF} t\right) \exp(jV_{DCx}) \right] \\
 &= E_c(t) \left[\sum_{n=-\infty}^{\infty} J_n(m_{RFx}) e^{jn\omega_{RF}t} + e^{j\varphi_x} \sum_{n=-\infty}^{\infty} j^n J_n(m_{RFx}) e^{jn\omega_{RF}t} \right] \approx 2E_c(t) [J_0(m_{RFx}) + J_1(m_{RFx}) e^{j\omega_{RF}t}]
 \end{aligned} \tag{1}$$

where $m_{RFx} = \pi A_x V_{RF} / 4 V_\pi$ represents the modulation index of the two PMs in the DMZMx. A_x is the attenuation coefficient of TAx. $\varphi_x = \pi V_{DCx} / V_\pi$ denotes the phase difference between the

two arms of the DMZMx that introduced by the DCx bias voltage. $J_n(\cdot)$ is the first kind of the Bessel function.

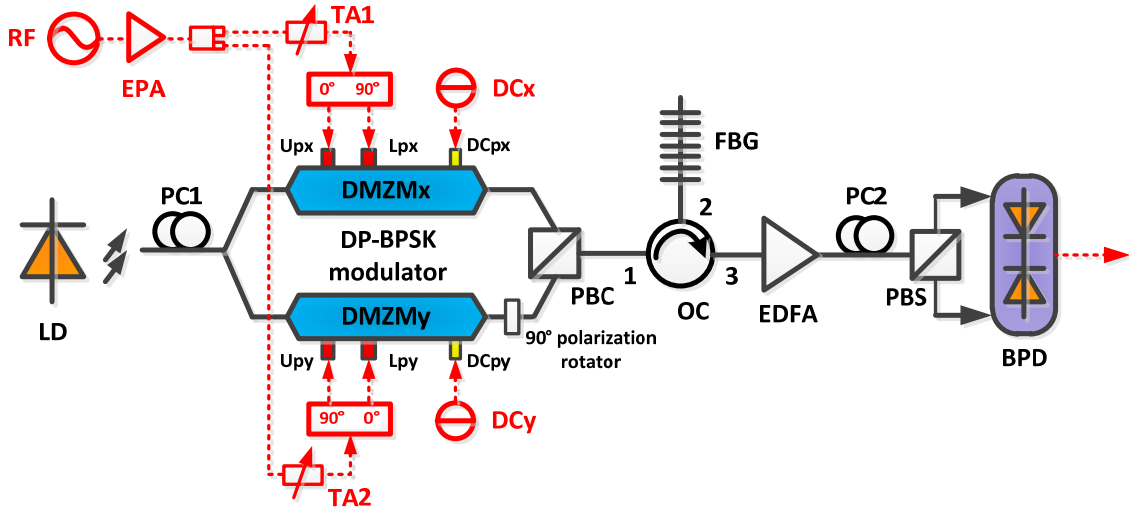


Fig. 1 The schematic of RF frequency based phase shifting system

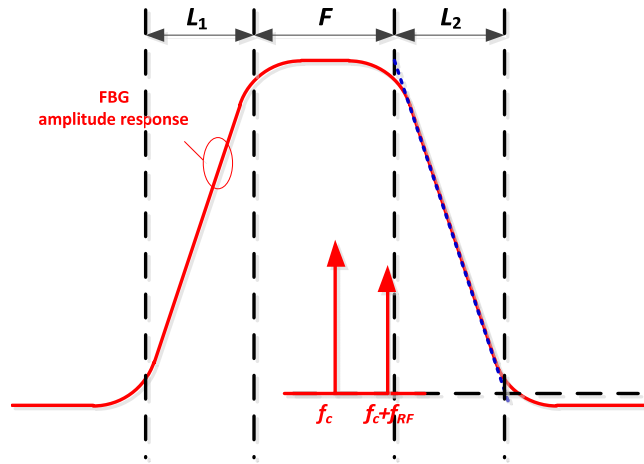


Fig. 2 The reflection spectrum of FBG

Similarly, the low-path RF signal is also split and phase shifted by the 90° hybrid coupler to drive the DMZMy. Differently, the 90° shifted one is introduced to the Uport, and

the non-shifted one is led to the Lport. The DC bias voltage is set to be $\pi/2$. Under the small signal modulation, the output of the DMZMy can be written as

$$\begin{aligned}
 E_{DMZMy}(t) &= E_c(t) \left[\exp\left(j \frac{A_y V_{RF}}{4} \cos \omega_{RF} t\right) + \exp\left(j \frac{A_y V_{RF}}{4} \sin \omega_{RF} t\right) \exp(jV_{DCy}) \right] \\
 &= E_c(t) \left[\sum_{n=-\infty}^{\infty} j^n J_n(m_{RFy}) e^{jn\omega_{RF}t} + e^{j\varphi_y} \sum_{n=-\infty}^{\infty} J_n(m_{RFy}) e^{jn\omega_{RF}t} \right] \approx 2E_c(t) [J_0(m_{RFy}) + jJ_1(m_{RFy}) e^{j\omega_{RF}t}]
 \end{aligned} \tag{2}$$

where $m_{RFy} = \pi A_y V_{RF} / 4 V_\pi$ represents the modulation index of the two PMs in the DMZMy. A_y is the attenuation coefficient of TAy. $\phi_y = \pi V_{DCy} / V_\pi$ denotes the phase difference between the two arms of the DMZMy that introduced by the DCy bias voltage. It can be seen from (1) and (2) that the optical carrier and the +1st order sideband are reserved. The signal from the DMZMy is polarized by the 90° polarization rotator before combined by the PBC. Because of the rotator, the two modulated signals from the two DMZMs are mutually orthogonal in the polarization states. Therefore, the output signal of the DP-BPSKM can be written as

$$E_{DP}(t) = E_{DMZMx}(t)\vec{e}_x + E_{DMZMy}(t)\vec{e}_y \quad (3)$$

$$E_{FBG}(t) = H(\omega)E_{DP}(t) = 2E_c \left\{ \begin{array}{l} J_0(m_{RFx})|H(\omega_c)|e^{j\omega_c t} e^{[j\arg H(\omega_c)]} \\ + J_1(m_{RFx})|H(\omega_c + \omega_{RF})|e^{j(\omega_c + \omega_{RF})t} e^{[j\arg H(\omega_c + \omega_{RF})]} \end{array} \right\} \vec{e}_x + 2E_c \left\{ \begin{array}{l} J_0(m_{RFy})|H(\omega_c)|e^{j\omega_c t} e^{[j\arg H(\omega_c)]} \\ + jJ_1(m_{RFy})|H(\omega_c + \omega_{RF})|e^{j(\omega_c + \omega_{RF})t} e^{[j\arg H(\omega_c + \omega_{RF})]} \end{array} \right\} \vec{e}_y \quad (4)$$

The reflected signal is then sent to the port2 and transferred to the Erbium Doped Fiber Amplifier (EDFA) from the port3 and the power is amplified. After that, the two polarized signals are aligned to the two principal axes in the polarization beam splitter (PBS) and are split into two branches (up-branch and

where \vec{e}_x and \vec{e}_y are the mutually orthogonal basic arrows. After that, the modulated signal is led to the optical circulator (OC) which possesses three ports (port1, port2, and port3). The lightwave goes through from port1 to port2 and reflected back by the FBG whose reflection function is $H(\omega)$. In this structure, the reflection spectrum of the FBG is adopted, and Fig. 2 shows the reflection spectrum. It is divided into three parts of L_1 band, F band and L_2 band. In the F band, the amplitude-frequency response is flat. However, in the L_1 and L_2 bands, the amplitude-frequency response shows approximately inverse proportion and direct proportion, respectively. Assume that the central angular frequency of the FBG is ω_B , the range of the F band is $\Delta\omega_F$, and the range of the L_1 and L_2 bands are all $\Delta\omega_L$. Therefore, the reflected signal can be expressed as

low-branch). They are impinged to the two photodiodes (PDx and PDy) in the balanced photodiode (BPD), respectively. Two microwave currents are then achieved, and they are inversely combined by the PBD. The output signal can be expressed as

$$I_{BPD}(t) = I_{PDx}(t) - I_{PDy}(t) = 8E_c R G^2 |H(\omega_c)| |H(\omega_c + \omega_{RF})| \left\{ \left[J_1(m_{RFx}) J_0(m_{RFx}) \times \cos(\omega_{RF}t + \arg H(\omega_c + \omega_{RF}) - \arg H(\omega_c)) \right] - \left[J_1(m_{RFy}) J_0(m_{RFy}) \sin(\omega_{RF}t + \arg H(\omega_c + \omega_{RF}) - \arg H(\omega_c)) \right] \right\} + D = 8\Psi E_c R G^2 |H(\omega_c)| |H(\omega_c + \omega_{RF})| \times \cos(\omega_{RF}t + \arg H(\omega_c + \omega_{RF}) - \arg H(\omega_c) + \Theta) + D \quad (5)$$

Here, R is the responsivity of the PD. G is the gain of the EDFA. $E_{FBGx}(t)$ and $E_{FBGy}(t)$ are the reflected signals in the two polarization states, respectively.

$$\Psi = \sqrt{[J_1(m_{RFx})J_0(m_{RFx})]^2 + [J_1(m_{RFy})J_0(m_{RFy})]^2} \quad (6)$$

$$\Theta = \tan^{-1} \left(\frac{J_1(m_{RFx})J_0(m_{RFx})}{J_1(m_{RFy})J_0(m_{RFy})} \right) \quad (7)$$

$$D = [J_0^2(m_{RFx}) - J_0^2(m_{RFy})] |H(\omega_c)|^2 + [J_1^2(m_{RFx}) - J_1^2(m_{RFy})] |H(\omega_c + \omega_{RF})|^2 \quad (8)$$

Equation (7) represents the phase shift of the recovered microwave signal consists of two components. One of them is the frequency dependent phase shift $\arg H(\omega_c) - \arg H(\omega_c + \omega_{RF})$, another one is the RF amplitude dependent phase shift Θ . It is obvious that when the RF amplitude is fixed, the frequency determines the phase shift. When the frequency is fixed, the RF amplitude ascertains the phase shift.

III. SIMULATION RESULTS AND DISCUSSION

A simulation based on the structure that shown in Fig. 1 is carried out by the commercial software of "Optisystem". A lightwave with the linewidth of 10 kHz is employed as an optical carrier. The frequency and the power of the lightwave are 193.11 THz and 10 dBm, respectively. It is first injected into the DP-BPSK modulator whose half-wave voltage is 4 V and the extinction ratio is 20 dB. The modulator is driven by a microwave signal, which is divided into four paths and phase

shifted by two 90° hybrid couplers. The separated microwave signals are fed to the four RF ports respectively to drive the modulator. After that, the modulated signal transfers through the OC and reflected by the specially designed FBG. The central frequency of the FBG is 193.1 THz, and the 1 dB bandwidth is about 20 GHz.

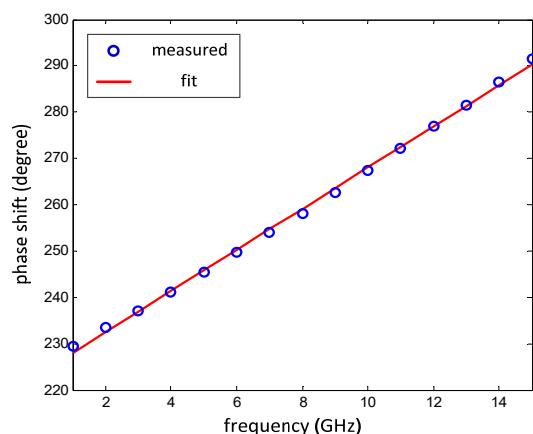


Fig. 3 The linear response result of the frequency dependent phase shifter

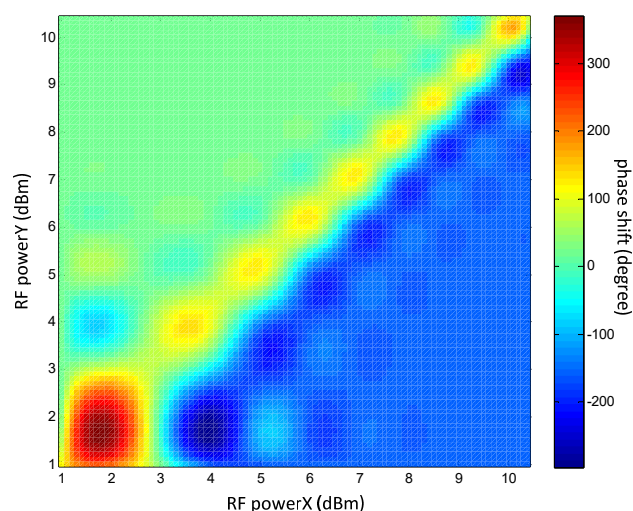


Fig. 4 The full range phase shift based on different RF power

In order to achieve the +1st order single sideband, the DC voltages (DCx and DCy) in the DP-BPSK should be properly settled. Based on the theoretical analysis before, the DCx and DCy are set to be -2 V and 2 V, respectively. At first, the amplitude of the microwave is set to be 0.1 V (6.99 dBm), and two attenuation coefficients are the same and fixed. With the frequency of the microwave signal tuned from 1GHz to 15 GHz, the phase of the recovered output signal is measured and shown in Fig. 3. After linear fitting based on the measured data, the result shows a high anastomosis to linear response. In addition, the RF power also makes contribute to the phase shift basing on the theoretical analysis before. In this work, the two attenuators are tuned to flexibly change the RF powers (RF powerX and RF powerY) those drive two DMZMs. According

to the simulation results that shown in Fig. 4, it can be figured that as the RF powerX and RF powerY changed respectively, the phase of the recovered output signal shows a full range of 0-360° shift. It exemplifies that when the frequency of the modulation signal is fixed, the phase shift can be fully tuned by adjusting the RF power. In this scheme, the influence of the distortion factors is investigated by measuring the spurious free dynamic range (SFDR). The two microwave signals with frequencies of 5 GHz and 5.01 GHz are employed to perform the two-tone test. Two attenuators are adjusted independently to investigate the SFDR. As Fig. 5 shows that when the input RF powerX increases from 6.99 dBm to 13.01 dBm, the power of the fundamental component and the 3rd-intermodulation distortion (IMD3) components keep increasing. The measured SFDR is about 70.90 dB·Hz^{2/3}. In the meantime, the RF powerY is also tuned and the SFDR is also measured. It can be seen in Fig. 6 that the SFDR is about 72.11 dB·Hz^{2/3}.

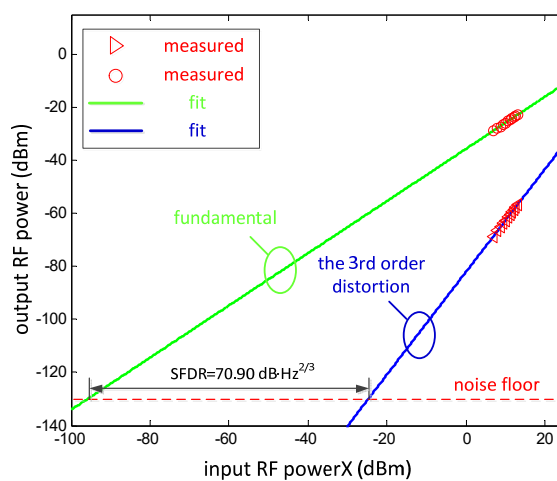


Fig. 5 The measured SFDR based on different input RF powerX

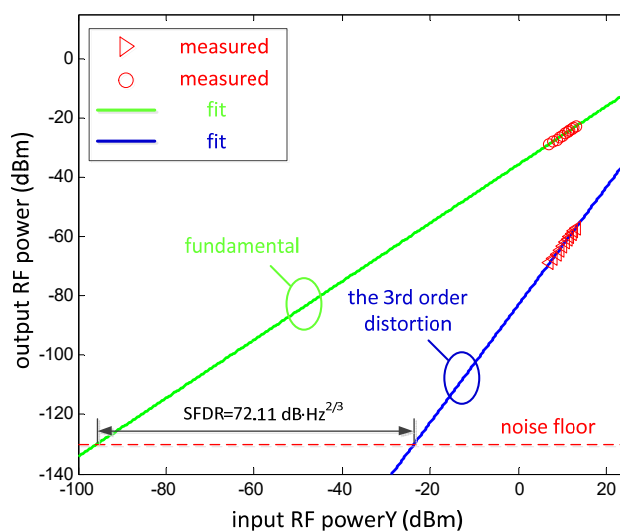


Fig. 6 The measured SFDR based on different input RF powerY

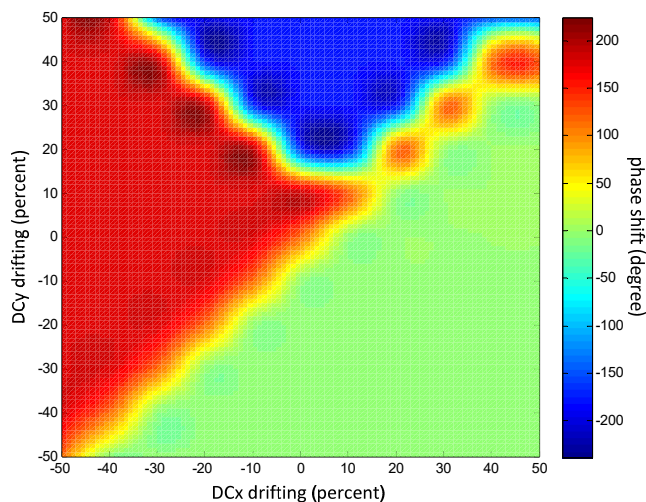


Fig. 7 The phase variation against the DC drifting

The key device in this scheme is the DP-BPSK modulator which is a kind of electro-optic modulator (EOM). DC drifting is a characteristic of the EOM due to the specially designed intensity interference structure. A serious DC drifting may greatly distort the final result. In this simulation, another work is carried to investigate how the DC drifting influences the phase of the recovered output signal. In practical, two DC bias voltages (DCx and DCy) in two DMZMs deviate from the settled values independently. Hence, the two DC bias voltages in this simulation platform are also changed respectively and the result is shown in Fig. 7. It can be figured that under the large deviation range (-50 percent to 50 percent), the phase of the recovered output signal also changes from -200 to 200. Such a sensitive reaction to the DC drifting requires a DC feedback circuit.

IV. CONCLUSION

In this paper, a frequency-dependent phase shifter with full tuning range of 0° - 360° is proposed and verified by the simulation. The key devices are the DP-BPSK modulator and the commercial FBG. The simulation results exemplify that when different microwaves with different frequencies drive the modulator, the phase shifter shows a linear response to different frequencies. Furthermore, the phase shift can also be tuned from 0° to 360° by adjusting the RF power. In addition, under different RF powerX and RF powerY, the SFDR of 70.90 dB \cdot Hz $^{2/3}$ and 72.11 dB \cdot Hz $^{2/3}$ are achieved. The simulation results also figure out the sensitive reaction of DC drifting which can be well improved by the DC feedback circuit. The full range tunable frequency-dependent phase shifter can be widely used to expand the operation bandwidth in phase array radar system.

ACKNOWLEDGMENT

This research was supported by the National Natural Science Foundation of China (No. 61571461), (No. 61231012) and (No. 61401502), Natural Science Foundation of Shaan Xi Province (No. 2016JQ6008).

REFERENCES

- [1] J. Capmany and D. Novak, "Microwave photonics combines two worlds", *Nature Photonics*, vol. 1, no. 6, pp. 319-330, Sep. 2007.
- [2] Jianping Yao "Microwave Photonics", *Journal of lightwave technology*, vol. 27, no. 3, pp. 314-335, Feb. 2009.
- [3] Xudong Wang, Erwin H. W. Chan, Robert A. Minasian, "Optical-to-RF phase shift conversion-based microwave photonic phase shifter using a fiber Bragg grating", *Optics Letters*, vol. 39, no. 1, pp.142-145, Jan. 2014.
- [4] Xudong Wang, Erwin H. W. Chan, Robert A. Minasian, "All-Optical Photonic Microwave Phase Shifter Based on an Optical Filter With a Nonlinear Phase Response", *Journal of lightwave technology*, vol. 31, no. 20, pp. 3323-3330, Oct. 2013.
- [5] Wei Li, Wen Hui Sun, Wen Ting Wang, Ning Hua Zhu "Optically controlled microwave phase shifter based on nonlinear polarization rotation in a highly nonlinear fiber", *Optics letters*, vol. 39, no. 11, pp. 3290-3293, Jun. 2014.
- [6] Xudong Wang, Jianxun Yang, Erwin H. W. Chan, Xinhua Feng, Baiou Guan, "Photonic microwave phase shifter based on dual-sideband phase-control technique", *Optics letters*, vol. 40, no. 15, pp. 3508-3511, Aug. 2015.
- [7] Yamei Zhang, Shilong Pan "Frequency-multiplying microwave photonic phase shifter for independent multichannel phase shifting", *Optics letters*, vol. 41, no. 6, pp. 1261-1264, Mar. 2016.
- [8] Weiyu Wang, Wenhui Sun, Wenting Wang et. al. "A wideband photonic microwave phase shifter using polarization-dependent intensity modulation", *Optics communications*, no. 356, pp. 522-525, Aug. 2015.
- [9] J. Yang, E. H. W. Chan, X. Wang, X. Feng, B. Guan, "Broadband photonic microwave phase shifter based on controlling two RF modulation sidebands via a Fourier-domain optical processor", *Optics express*, vol. 23, no. 94, pp. 12100-12110, May 2015.
- [10] A. Loayssa and F. J. Lahoz, "Broad-band RF photonic phase shifter based on stimulated Brillouin scattering and single-sideband modulation," *IEEE Photon. Technol. Lett.*, vol. 18, no. 1, pp. 208-210, Jan. 2006.
- [11] W. Li, N. H. Zhu, L. X. Wang, and H. Wang, " Broadband phase-to-intensity modulation conversion for microwave photonics processing using Brillouin-assisted carrier phase shifter, " *J. Lightw. Technol.*, vol. 29, no. 24, pp. 3616-3621, Dec. 2011.
- [12] Tianwei Jiang, Song Yu, Ruihuan Wu, Dongsheng Wang, Wanyi Gu "Photonic downconversion with tunable wideband phase shift", *Optics letters*, vol. 41, no. 11, pp. 2640-2643, Jun. 2016.
- [13] T. Li, E. H. W. Chan, X. Wang, X. Feng, B. Guan, "All-Optical Photonic Microwave Phase Shifter Requiring Only a Single DC Voltage Control" *Photonics Journal*, vol. 8, no. 4, pp. 1-10, Aug. 2016.
- [14] Vanessa C. Duarte, Miguel V. Drummond, Rogério N. Nogueira, "Photonic True-Time-Delay Beamformer for a Phased Array Antenna Receiver based on Self-Heterodyne Detection", *Journal of lightwave technology*, vol. 34, no. 23, pp. 5566-5575, Dec. 2016.
- [15] C. Ta-Shun and H. Hashemi, "True-time-delay-based multi-beam arrays," *IEEE Trans. Microw. Theory Techn.*, vol. 61, no. 8, pp. 3072-3082, Aug. 2013.

Yufu Yin is the headmaster of College of Information and Navigation, Air Force Engineering University. He is also the professor that interests in wireless communication.

Tao Lin received the B.E. degree from the College of Information and Navigation, Air Force Engineering University, Xi'an, China, in 2015. After that, he continued to achieve the M. S. degree from the College of Information and Navigation, Air Force Engineering University, Xi'an, China, in 2015, where he is currently working toward the Ph.D. degree. His current research interests include optical frequency-comb generation and photonic microwave frequency conversion.

Shanghong Zhao received the B.S. and M.S. degrees from the Physics Department, Lanzhou University, Lanzhou, China, in 1984 and 1989, respectively, and the Ph.D. degree from Xi'an Institute of Optics and Precision Mechanics of CAS in 1998. He is currently a Full Professor in the School of Information and Navigation, Air Force Engineering University, Xi'an, China. His research interests include laser technology, optical satellite communication, and networking.

Zihang Zhu received the B.E., M.E., and Ph.D. degrees from the Air-to-Ground Communication Department, Telecommunication Engineering

College Air Force Engineering University, Xi'an, China, in 2007, 2009, and 2015, respectively. He is currently a Lecturer in the School of Information and Navigation, Air Force Engineering University. His research interests include photonic generation of microwave signals, intersatellite microwave photonics links, and radio-over-fiber systems.

Xuan Li received the B.E. and M.E. degrees in 2011 and 2014, respectively, from the School of Information and Navigation, Air Force Engineering University, Xi'an, China, where he is currently working toward the Ph.D. degree. From March 2015 to June 2016, he was with the Microwave Photonics Research Laboratory, College of Electronic and Information Engineering, Nanjing University of Aeronautics and Astronautics, Nanjing, China. His current research interests include arbitrary waveform generation and signal processing.

Wei Jiang received the B. E. degree from Sichuan University, Chengdu, China, in 2000, and the M. S. degree from China Academy of Space Technology (CAST), Xi'an, China, in 2007. She is currently a Senior Engineer in the National Key Laboratory of Science and Technology on space Microwave, CAST, Xi'an. Her current research interests include microwave photonics and optical channelization.

Hui Wang is now working toward the B. E. degree in the College of Information and Navigation, Air Force Engineering University, Xi'an, China.